

Measurement of longwave radiative properties of energy-saving greenhouse screens

Adeel Rafiq,¹ Wook Ho Na,² Adnan Rasheed,² Jong Won Lee,³ Hyeon Tae Kim,⁴ Hyun Woo Lee^{1,2}

¹Department of Agricultural Engineering, Kyungpook National University, Daegu; ²Smart Agriculture Innovation Center, Kyungpook National University, Daegu; ³Department of Horticulture Environment System, Korea National College of Agriculture and Fisheries, Jeonju-si; ⁴Department of Bio-Industrial Machinery Engineering, Gyeongsang National University, Jinju, Republic of Korea

Abstract

Light intensity, temperature, and humidity are key factors affecting photosynthesis, respiration, and transpiration. Among these factors, temperature is a crucial parameter to establish an optimal greenhouse climate. Temperature can be controlled by using an appropriate climate screen, which has a considerable impact on crop quantity and quality. The precise measurements of longwave radiative properties of screens are vital to the selection of the most suitable screen for greenhouses so that the desired temperature and a favorable environment can be provided to plants during nighttime. The energy-saving capability of screens can also be calculated by using these properties as inputs in a physical model. Two approaches have been reported so far in the literature for the measurement of these properties, *i.e.*, spectrophotometry and wideband radiometry. In this study, we proposed

some modified radiation balance methods for determining the total hemispherical longwave radiative properties of different screens by using wide-band radiometers. The proposed method is applicable to materials having zero porosity, partial opacity, and asymmetric screens with 100% solidity. These materials were not studied previously under natural conditions. The existing and proposed methods were applied and compared, and it was found that the radiometric values obtained from the developed methodology were similar to those previously reported in the literature, whereas the existing method gave unstable results with zero reflectance.

Introduction

Growing greenhouse plants is a complicated process that involves selecting suitable energy-saving materials and procedures on a large scale that are strongly affected by the conditions of the outside environment, the greenhouse, and the plant itself. Considering that the exterior conditions are unchangeable, plant transpiration is influenced by numerous factors (Svensson, 2014). Photosynthesis, respiration, and transpiration are the fundamental processes of plant growth and development, which depend predominantly on light intensity, temperature, and humidity (Gernot, 2008; Beyl and Trigiano, 2011).

In winter, heating is a critical part of greenhouse farming, as it is necessary to achieve the required optimal temperature for crop growth (Sethi *et al.*, 2013; Rasheed *et al.*, 2018a). When designing a greenhouse, the selection of appropriate materials can positively impact energy requirements and fuel consumption (Ponce *et al.*, 2014; Marshall, 2016; Rasheed *et al.*, 2018b).

Shading is one of the cheapest methods used by producers to moderate solar heat load on greenhouses, which removes the superfluous solar radiation during summer periods. The materials utilized for shading can also be used for thermal insulation in winter (Willits and Peet, 2000; Chen *et al.*, 2011). Shading is usually performed by using porous materials such as cloths and plastic nets, or by spraying white lime on the outside surface of the greenhouse, glazing, and filling with polystyrene balls in acrylic channel greenhouses (Al-Helal and Al-Musalam, 2003).

Generally, the thermal screens used in greenhouses during the winter season to minimize heat loss at nighttime can also be utilized for shading during the summer season (Shukla *et al.*, 2008). Numerous methods have been employed to determine the properties of screens. Nevertheless, two main approaches exist. The first is based on the integration of monochromatic light measurements (using spectrophotometers) for the probable spectrum under which the screen is to be used (Simpkins *et al.*, 1976; Nijkskens *et al.*, 1985; Nijkskens *et al.*, 1989; Cohen *et al.*, 2014). When applied

Correspondence: Hyun Woo Lee, Department of Agricultural Engineering, Kyungpook National University, Daegu 41566, Republic of Korea. Tel.: +82.53.950.5736. E-mail: whlee@knu.ac.kr

Key words: Emittance; net radiometer; pyrgeometer; sky temperature; solidity; transmittance.

Funding: this work was supported by the Korea Institute of Planning and Evaluation for Technology in Food, Agriculture, Forestry and Fisheries through the Agriculture, Food and Rural Affairs Convergence Technologies Program for Educating Creative Global Leader, funded by the Ministry of Agriculture, Food and Rural Affairs (MAFRA) (717001-7). This research was supported by Basic Science Research Program through the National Research Foundation of Korea (NRF) funded by the Ministry of Education (NRF-2019R111A3A01051739).

Conflict of interests: the authors declare no potential conflict of interests.

Received for publication: 24 May 2021.
Accepted for publication: 12 July 2021.

©Copyright: the Author(s), 2021

Licensee PAGEPress, Italy

Journal of Agricultural Engineering 2021; LII:1209

doi:10.4081/jae.2021.1209

This article is distributed under the terms of the Creative Commons Attribution Noncommercial License (by-nc 4.0) which permits any non-commercial use, distribution, and reproduction in any medium, provided the original author(s) and source are credited.

precisely, this method gives standard values that are reportedly cataloged by the European Economic Community (Nijskens *et al.*, 1985). In contrast, the properties of a screen can be calculated for a specific waveband, *i.e.*, photosynthetically active radiation and short and longwave bands (Godbey *et al.*, 1979; Bailey, 1981; Yates, 1986; Castellano *et al.*, 2010; Abdel-Ghany and Al-Helal, 2012; Cohen *et al.*, 2014), using wideband radiometers (Castellano *et al.*, 2006). It is impractical to measure the longwave transmittance and reflectance precisely because the transmitted and reflected diffuse longwave radiations from the screen would have the same directional characteristics as the diffuse emission, and all the components of the received radiation cannot be separated from the transmission or reflection components (Abdel-Ghany and Al-Helal, 2012). Another problem is the instability of screen properties (Cohen *et al.*, 2012). When screens are exposed to outdoor conditions, they may change considerably during their lifetime, as seen in previous studies. Bailey (1981) showed that abrasion increased the emissivity of a screen, while Meijer (1980) reported a decrease in screen emissivity after being exposed for 10 months. The accumulation of dust on a screen has a significant impact on the transmission value, with reported reductions as high as 17% (Tanny, 2006). Therefore, a mathematical model is essential to determine these properties with readily available equipment in conditions close to those under which the screens are normally used. To address these issues, Abdel-Ghany *et al.* (2016) and Cohen and Fuchs (1999) presented a radiation balance method for the measurement of the longwave radiative properties of shading nets and thermal screens under natural conditions. Nighttime experiments involved placing a sample screen between the open sky and a black surface. Different cases were described for various materials, but they were still limited to specific materials. Furthermore, the mathematical model given by Cohen and Fuchs (1999) requires several input parameters for a screen composed of more than one material, *i.e.*, reflectance, emittance, transmittance, and porosity of each material separately along with incoming and outgoing radiations and surface temperature, which makes it difficult to use.

Abdel-Ghany *et al.* (2016) described a simplified model that used basic incoming and outgoing radiations with the screen and black-cloth surface temperatures as input parameters in the model equations, which make it flexible and easy to use. However, the problem with this methodology is that it does not consider the entirety of longwave incoming radiations (Q_4) from the black cloth toward the screen in its radiation balance equations. Instead, this approach only involves the emissive power of the black cloth (E_b) in the model equations, which undermines the reflectivity of the screen.

In this study, we describe modified radiation balance equations involving the emissive power of the black cloth for different types of materials that consider all the longwave radiations (Q_4). Furthermore, depending on the physical properties of the materi-

als, new equations are developed. The newly proposed methods do not require much information about the materials to calculate radiative properties, as described by Cohen and Fuchs (1999). Particularly, we sought to develop new methods that can be used with cheap radiometers and can measure the properties of samples with diverse screen types without involving any error or technical expertise. Our current methodology focuses on developing generalized energy balance equations without dealing with specific materials and is also compared with the previous methodology. The samples selected were representative materials of various commercial screens. Our previous studies (Rafiq *et al.*, 2019, 2020) developed radiation balance equations for materials that are widely used by farmers in Korea (not emphasizing the development of a general methodology). These studies characterized the relationship between absorbed and emitted radiation and also determined the heat transfer coefficient. These methodologies allow researchers to use energy balance equations for real-time energy-saving measurements by using a building energy simulation model to determine whether a screen is a good heat insulator or conductor under natural environmental conditions (Rasheed *et al.*, 2020).

A mid-infrared region (2.5–25 μm) spectrophotometer (Fourier transform-infrared/near infrared) was used to validate the output obtained by the proposed radiation balance equations. The results of the proposed method for transparent, semitransparent, and porosity materials were analyzed, and the results of the former two materials were also compared with those of the existing methodology developed by Abdel-Ghany *et al.* (2016) to show the difference between the two procedures.

Materials and methods

The physical properties and the composition of the tested materials are presented in Table 1. During the daytime, Tempa 8672 D FB reflects the sunlight and diffuses it to reduce the temperature increase caused by the greenhouse effect. During the nighttime, it facilitates heat retention and maintains a steady temperature, which saves energy. The main function of Luxous-1347 D FR is saving energy by maximizing light transmission. White polyester is a domestic product that is widely used as an insulating screen. Polyethylene is a predominantly plastic film that is preferred by the majority of farmers due to its affordability, flexibility, and simple manufacturing. In our study, in order to confirm the results obtained by the proposed method when characterizing transparent and porous materials, we used polyethylene as a reference material due to its well-known properties. This research was carried out on the roof of a building to obtain unimpeded sky radiation. A hollow wooden frame was made for the investigation. The bottom part of the frame was covered with black cloth with known

Table 1. Properties of the sample screen and film.

Sample screen	Weight (g/m ²)	Thickness (mm)	Properties Energy-saving (%)	Composition
Tempa 8672 D FB	79	0.25	72	57% Aluminum 43% Polyester
Luxous-1347 FR	58	0.22	47	100% Polyester
White polyester	140	0.25	-	100% Polyester
Polyethylene film	84	0.07	-	100% Polyethylene

radiometric properties ($\tau_b = 0$, $\rho_b = 0.07$, $E_b = 0.93$). The setup volume was 3.12 m^3 ($2.4 \text{ m width} \times 2.6 \text{ m length} \times 0.5 \text{ m height}$). The dimensions of the setup and the positions of the equipment are illustrated in Figure 1. The simplified graphic representation in Figure 2 depicts the radiation exchanged between the sky, the material tested, and the black cloth. The unknown parameters are highlighted in red in the figure. The downward and longwave radiations (Q_1 and Q_3) were measured with a pyrgeometer, whereas the upward fluxes (Q_2 and Q_4) were computed from the difference between the net radiometer indication and the values of the downward fluxes. Two thermocouple wires were used to measure the surface temperature of the black cloth. All the measured parameters were recorded at 10-min intervals and saved in a data logger. Information about the equipment and data loggers can be found in Table 2.

The outgoing longwave radiation equation above the screen surface (Q_2) for symmetric materials (both sides are similar) is given below in units of W/m^2 .

$$Q_2 = E_n + \rho_n Q_1 + \tau_n Q_4, \quad (1)$$

where ρ_n is the reflectance of the screen, E_n is the emissive power of the screen in W/m^2 , τ_n is the transmittance of the screen, and Q_1 is the downward sky radiation in W/m^2 .

The outgoing longwave radiation equation over the black surface (Q_3) and below the screen surface for symmetric materials is given below in units of W/m^2 .

$$Q_3 = E_n + \tau_n Q_1 + \rho_n Q_4 \quad (2)$$

The reflected portion of the incoming longwave radiation toward the screen and above the black cloth (Q_4) depends upon the physical condition of the screen. If the screen has a small porosity (less than 0.05), then $\tau_n \rho_b Q_1$ is neglected in the formation of Q_4 . It was ignored because when 5% (or less than 5%) of ' $\tau_n Q_1$ ' strikes the black cloth (93% absorbance), it disappears. The equation of Q_4 for such materials is given below in units of W/m^2 .

$$Q_4 = E_b + \rho_b E_n + \rho_n \rho_b Q_4, \quad (3A)$$

where ρ_b is the reflectance of the black cloth, and E_b is the emissive power of the black cloth in W/m^2 , which is determined by the Stefan-Boltzmann law.

The incoming radiation (Q_4) for the transparent, semitransparent, and partial-porosity materials is given below in units of W/m^2 .

$$Q_4 = E_b + (\rho_b + \mu)E_n + (\rho_b - \mu)\rho_n Q_4 + (\rho_b - \mu)\tau_n Q_1 \quad (3B)$$

In the aforementioned case (3B), the reflection of all three components (E_n , $\rho_n Q_4$, and $\tau_n Q_1$) from the surface of the black cloth is considered, as $\tau_n Q_1$ will reach the surface of the black cloth due to the porosity or transparency of the sample. Q_4 will also reach the black cloth due to the presence of opaque material, such as the thread. While solving the three equations (1, 2, and 3B) using Matlab's iteration method, equation (3B) causes compatibil-

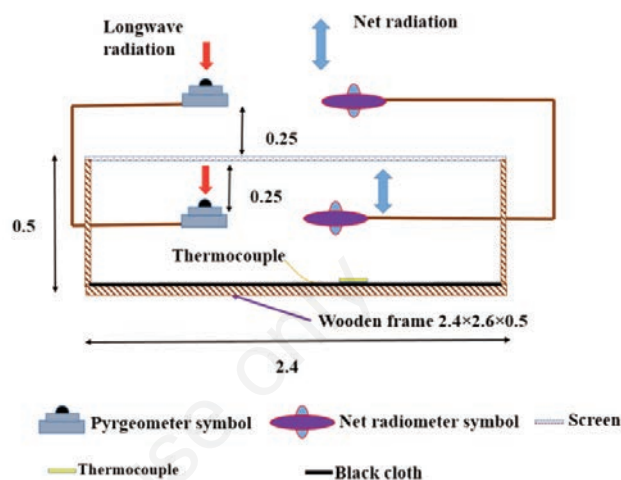


Figure 1. Sketch of the experimental setup, dimensions in [m], not to scale.

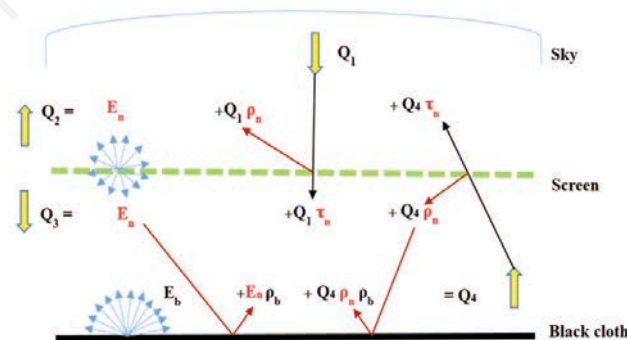


Figure 2. Ideal illustration of the incoming (Q_1 and Q_4) and the outgoing (Q_2 and Q_3) radiation from the screen.

Table 2. List of measuring sensors.

Parameter	Unit	Sensors	Range	Data logger
Net longwave radiation	W/m^2	NR Lite2 net radiometer (Kipp and Zonen, Netherlands)	0.2-100 μm	LR 5041 (Hioki, Japan)
Downward longwave radiation (Q_1)	W/m^2	CGR3 Pyrgeometer (Kipp and Zonen, Netherlands)	4.5-42 μm	21x Micrologger (Campbell Scientific, Inc. USA)
Downward longwave radiation (Q_3)	W/m^2	IR02 Pyrgeometer (Hukseflux, Netherlands)	4.5-40 μm	CR300 (Campbell Scientific, Inc. USA)
Temperature/relative humidity	$^{\circ}\text{C}\%$	Hobo pro v2 U23-002 (Onset, USA)	-40°C - 70°C 0%-100%	Hobo pro v2 U23-002 (Onset, USA)
Surface temperature	$^{\circ}\text{C}$	T-type thermocouple wires	-270°C - 370°C	Hobo UX120-014M (Onset, USA)

ity issues even though the number of equations is equal to the number of unknowns. In order to make these equations compatible to be solved simultaneously, μ (10^{-6}) is subtracted from the reflected portion of $\tau n Q_1$ and $\rho n Q_4$, and the same number is added into the reflected portion of E_n in Equation (3B). Micro (μ) is the smallest assumed number as the tolerance for the reflectance of the black cloth (ρb), which has no significant effect on the value, but aids in solving these equations. The subtraction and addition are based on radiation strength.

Kirchhoff's law of thermal radiation gives the following equation:

$$\tau n + \rho n + \epsilon n = 1, \quad (4)$$

where ϵn is the emittance of the screen. Equations (1), (2), and (3B) are used for polyethylene (transparent material) and Luxous-1347 (semitransparent material). The existing radiation balance method (ERBE) for transparent, semitransparent, or materials having partial porosity suggested by Abdel-Ghany *et al.* (2016) considers the emissive power of the black cloth, E_b , in Equations (1) and (2) instead of the entire radiation coming from the black cloth (Q_4). Moreover, this method does not take into account the reflection of $\rho n Q_4$ in the formation of Q_4 . Overestimation of the transmission leading to little or no reflection is a possible drawback of this hypothesis. Equations (1), (2), and (3A) were used for white polyester, as this material has low porosity. Tempa is an asymmetric material (both sides are different) with seven aluminum (opaque) and one transparent diffusion strips. The radiometric properties of the dull side of Tempa were determined by Equations (2), (3A), and (4). Similarly, the properties of the shiny side can be determined by simply flipping the side. However, in this study, we measured only the properties of the dull side. In this way, three equations were selected from the aforementioned cases based on the type of material to determine the radiometric properties of all the materials under natural conditions. Matlab and Excel were used to solve the above equations for E_n , τn , and ρn . The multiple reflections (ρn_2 , ρn_3 and ρb_2 , ρb_3) of thermal radiation between the screen and the black cloth were ignored. No angular interaction between the sample materials and the incident radiation was considered.

Solidity is defined as the ratio between the solid portion and the total area of a screen. This parameter can be used to calculate the convective heat transfer coefficient and is also helpful in the calculations of the radiometric properties of screens. Its measurement is important because it affects the radiometric properties of the materials. Three methods are currently available for the measurement of solidity (Cohen *et al.*, 2012). The first method is based on the radiation balance equation, the second is based on the interception of direct solar radiation, and the third is based on image processing. In this investigation, the image processing method was employed, as it was less time-consuming than the other two methods. ImageJ software was utilized for further processing of the images, which is a freely available source Java image processing program inspired by NIH Image that can compute the area and pixel value statistics of user-defined selections. Furthermore, it can measure distances and angles. For image processing, the first screens were tacked to a small frame (4×4 cm) and scanned at 300 dpi resolution with a flatbed scanner (Scanjet 5550c, HP, USA). The scanned images were then converted into black-and-white images by changing the image type to 8-bit and using a bandpass filter. The set scale command was used to adjust the image scale. These steps were prerequisites for the real and accurate measurement of the area. Thresholding and particle analyzing commands

were used to measure the empty areas of the images. The ratio between the empty and the total areas was taken for each material to measure the porosity. Then, the values of porosity were subtracted from 1 to obtain the solidity values.

Results and discussion

Weather conditions, particularly rainy nights and dense cloud cover, can affect the sensor reading, which ultimately changes the true results. To overcome such problems, several nights of experiments (as many as three) were repeated for a material to account for the environmental impact on the material and sensors. The results presented here are only for one dry and clear night. The impact of relative humidity on emissivity was reported in Cohen and Fuchs (1999). The reference study showed that when the relative humidity exceeded 85%, the emissivity value tended to increase with an increase in relative humidity. The impact of temperature on transmission and reflection was reported in Abdel-Ghany and Al-Helal (2012). This study discovered that temperature had an inverse relationship with transmittance and a direct relationship with reflectance, because as the night passes, the temperature decreases, which reduces the porosity of the material and affects its properties. The increase in relative humidity for each material can be seen in Figure 3, but this increase did not exceed 85%. A decrease in the ambient nighttime temperature of 2°C-5°C

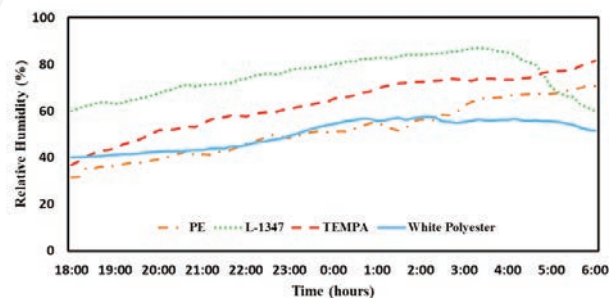


Figure 3. Relative humidity recorded during the experiment for each material.

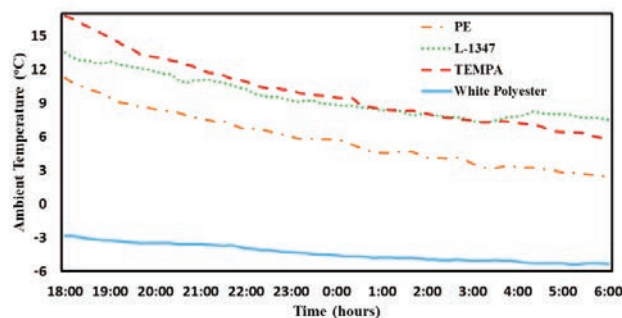


Figure 4. Ambient temperature recorded during the experiment for each material.

during the experiments for each material is shown in Figure 4.

The basic radiation parameters for polyethylene are depicted in Figure 5. During this experiment, we observed that the sky radiation (Q_1) was always less than the downward longwave radiation over the black surface (Q_3). The net radiometer readings were always negative, i.e., $Q_2 > Q_1$ and $Q_4 > Q_3$. The variation of the sky and ambient temperature for the first three days of November is presented in Figure 6. The sky temperature was calculated by using sky radiation data. An approximate difference of 20°C was observed between the sky and ambient temperatures in a previous study (Na *et al.*, 2013). In the present study, we found the maximum difference between the sky and ambient temperature to be 23.10°C; the minimum was 18.34°C. This setup functioned even when the ambient temperature variation was from -3°C to -5°C for white polyester. Such measurements were helpful to determine whether the equipment was working correctly or not. For the validation of the equations developed for transparent or partially porous materials, polyethylene was used as reference material. Table 3 shows a comparison of the transmittance of polyethylene measured by the proposed radiation balance method (PRBQ) and

ERBE method with the literature values and the spectrophotometer results obtained during this study. The outputs of the PRBQ and the spectrophotometer were identical for polyethylene, and both results are also in agreement with those of previous studies (Nijskens *et al.*, 1989; Papdakis *et al.*, 2000; Schettini *et al.*, 2007).

The output of the ERBE yielded a transmission of 71% for polyethylene, which is 16% greater than the standard literature value. Figures 7 and 8 illustrate the transmittance of the polyethylene film, white polyester, and Luxous-1347, measured spectrophotometrically. The PRBQ yielded a transmission of 2% for the white polyester, which was closer to the output values obtained by the spectrophotometer and validated the proposed model. The radiometric properties of Luxous-1347, measured by the PRBQ, were similar to those established in earlier works (Hemming *et al.*, 2017). Minor discrepancies due only to the placement of the measuring sensor were present. The difference in the transmission value due to the difference in the location of the sampling points measured by the spectrophotometer is shown in Figure 8. The radiometric properties of Luxous-1347 and polyethylene obtained from the ERBE and PRBQ *versus* time (from 18:00 to 6:00 o'clock) are dis-

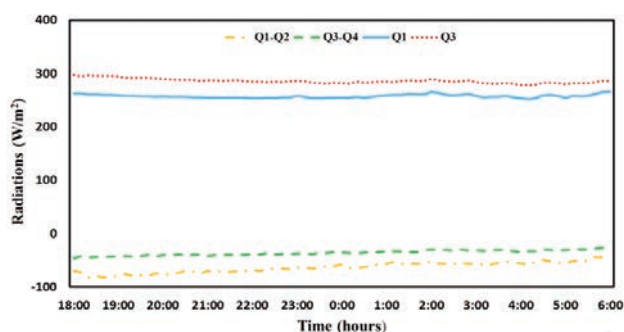


Figure 5. Basic radiation parameters for polyethylene.

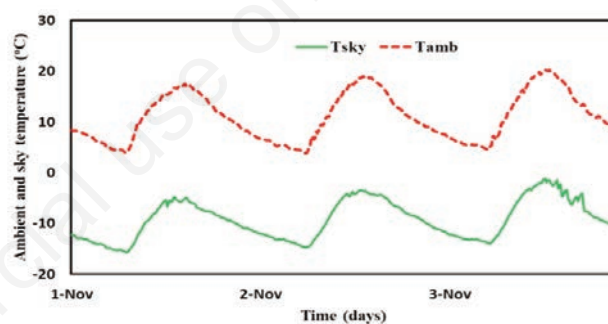


Figure 6. Variation of the ambient and sky temperatures.

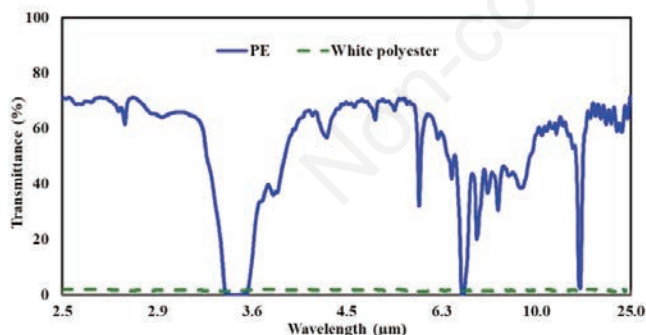


Figure 7. Variations in the transmittance of the screen and the film with wavenumber.

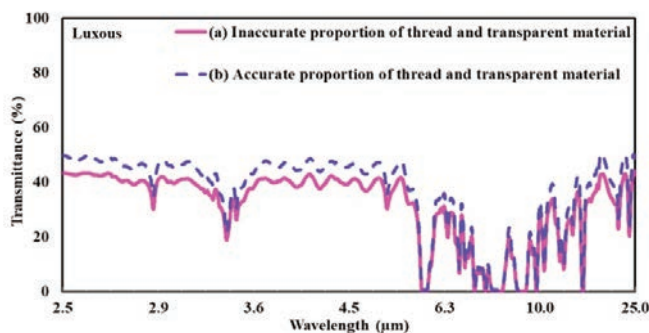


Figure 8. Discrepancy in transmission value due to the difference in location of sampling points.

Table 3. Comparative data of polyethylene transmittance.

Transmittance	0.550	0.545	0.610	0.550	0.550	0.539	0.710
Wavelengths (µm)	4.5-40	2.5-25	2.5-50	7-14	2.5-40	2.5-25	4.5-40
Reference	PRBQ	Present study	Papadakis <i>et al.</i> (2000)	Nijskens <i>et al.</i> (1989)		Schettini <i>et al.</i> (2007)	ERBE
Approach	RB	SP	SP	SP	SP	RB	

PRBQ, proposed radiation balance method; ERBE, existing radiation balance method; RB, radiation balance method; SP, spectrophotometer.

played in Figures 9 and 10, respectively, while Figure 11 shows the radiometric properties of the white polyester and Tempa obtained from the PRBQ. The results showed that even though the ambient temperature decreased, it had no significant impact on the radiometric properties, because the solidity was nearly 1 for the white polyester and exactly 1 for the other tested materials. Also, relative humidity did not show any effect on the emissivity of the tested materials, as it did not exceed the limit described in Cohen and Fuchs (1999). A comparison of the average radiometric properties of the tested materials obtained from the ERBE, PRBQ, and spectrophotometer measurements are listed in Table 4. During this experiment, Tempa and the white polyester showed the lowest transmission, because most of the areas of these two materials were opaque. The emittance and reflectance of the dull side of Tempa were similar to the values reported in Cohen and Fuchs (1999) for aluminum. Small differences in the calculated values were present due to the small transparent strip of Tempa. The white polyester showed the highest emittance as compared to those of the other materials and very low reflectance. White-colored materials have a high reflectance in the shortwave region and a high absorption or emittance for longwave radiation (Kishore, 2010). In the present study, we obtained low values of polyethylene reflectance.

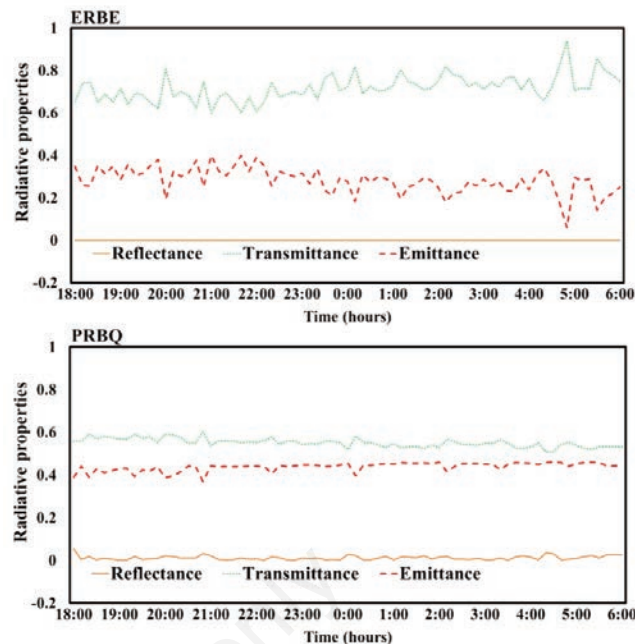


Figure 10. Radiative properties of polyethylene with the existing radiation balance method (ERBE) and proposed radiation balance method (PRBQ).

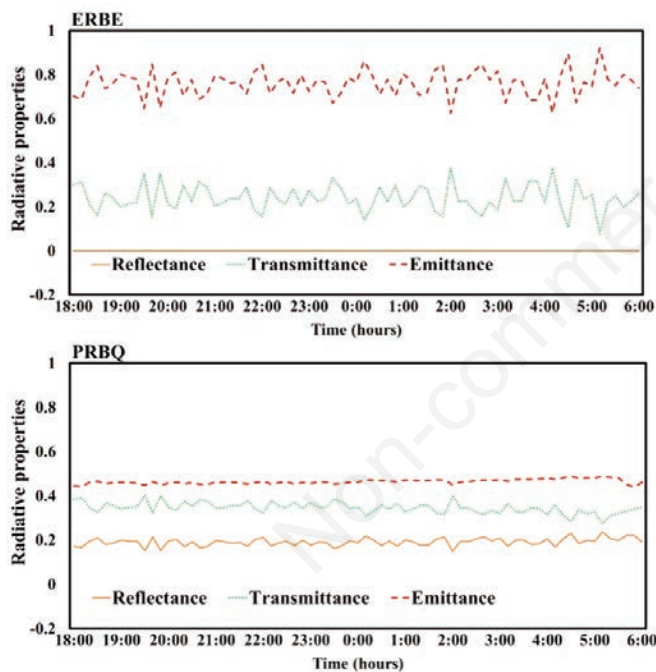


Figure 9. Radiative properties of Luxous-1347 with the existing radiation balance method (ERBE) and proposed radiation balance method (PRBQ).

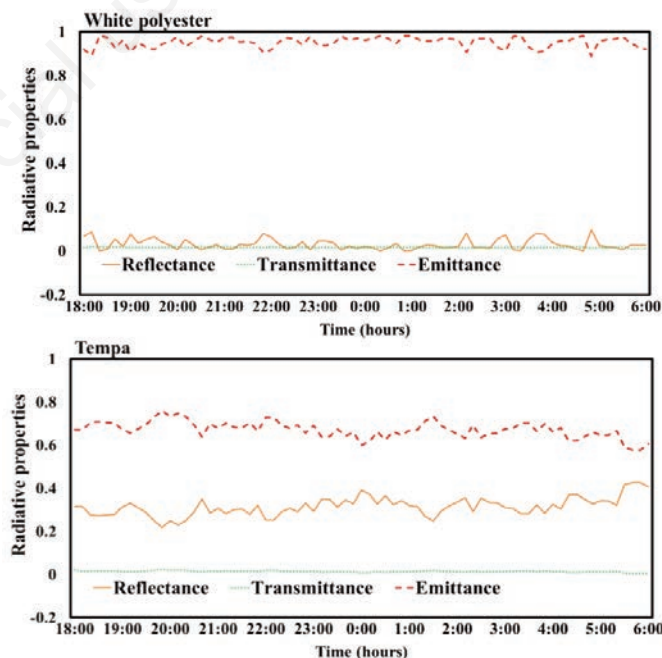


Figure 11. Radiometric properties of White polyester and Tempa, measured by the proposed radiation balance method.

Table 4. Average radiative properties of the tested materials.

Materials	Radiative properties			Solidity
	Emittance PRBQ	Emittance ERBE	Transmittance ERBE Spectrophotometer	
Polyethylene	0.44±0.02	0.29±0.06	0.55±0.02	1
Tempa 8672	0.67±0.04	N.A.	0.01±0.003	1
Luxous-1347	0.46 (0.47) ^o	0.76±0.05	0.34±0.03 (0.33) ^o	1
White polyester	0.94±0.02 (0.88) [*]	N.A.	0.02±0.001	0.99

PRBQ, proposed radiation balance method; ERBE, existing radiation balance method. ^{*}Value was suggested by Kim *et al.* (2009); ^ovalues were suggested by Hemming *et al.* (2017); N.A., not available.

Similar low reflectance values of different materials made of special high-density polyethylene have also been reported (Gentle *et al.*, 2013; Abdel-Ghany *et al.*, 2015).

Conclusions

The instability of screen properties due to dust accumulation, long-term exposure, and abrasion can lead to a significant change in the energy flux exchange. To overcome these issues, it is necessary to develop a mathematical model that can be used with readily available equipment. Various studies have been published that developed such models, but they were problematic as they required several input parameters and demanded high technical expertise, while other studies developed simplified models, but with limited applications.

Therefore, in this study, we proposed a radiation balance method that required a simple input of parameters, including incoming radiation, outgoing radiation, and the emissive power of black cloth, to measure the radiometric properties of materials. The results obtained by the PRBQ yielded less than a 1%-3% variation compared to the standard values, whereas their comparison showed that the ERBE output exhibited relatively considerable differences of approximately 15%-22% compared to the standard results. These appreciable differences were only due to having disregarded the first-order reflection of the materials with partial porosity. The excellent set of mathematical equations of the PRBQ are thus expected to be applied in measuring radiative properties of energy-saving screens and other films used in greenhouses under natural conditions, while requiring less technical expertise and yielding more accuracy under clear sky conditions.

Notation

PRBQ	= Proposed radiation balance method
ERBE	= Existing radiation balance method
Q_1	= Downward sky radiation in W/m^2
Q_2	= Outgoing longwave radiation above the screen surface in W/m^2
Q_3	= Outgoing longwave radiation over the black surface in W/m^2
Q_4	= Incoming longwave radiation toward the screen above the black cloth in W/m^2
E_b	= Emissive power of the black cloth in W/m^2
E_n	= Emissive power of the screen in W/m^2
τ_n	= Transmittance of the screen
τ_b	= Transmittance of the black cloth
ρ_n	= Reflectance of the screen
ϵ_n	= Emittance of the screen
ρ_b	= Reflectance of the black cloth
PE	= Polyethylene
N.A.	= Not applicable

References

- Abdel-Ghany A.M., Al-Helal I.M. 2012. A method for determining the long-wave radiative properties of a plastic shading net under natural conditions. *Sol. Energy Mater. Sol. C.* 99:268-76.
- Abdel-Ghany A.M., Al-Helal I.M., Shady M.R. 2015. On the emissivity and absorptivity of plastic shading nets under natural conditions. *Adv. Mech. Eng.* 7:1-9.
- Abdel-Ghany A.M., Al-Helal I.M., Shady M.R. 2016. Estimating the thermal radiative properties of shading nets under natural outdoor conditions. *J. Heat Transfer.* 138:1-6.
- Al-Helal I.M., Al-Musalam I.M. 2003. Influence of shading on the performance of a greenhouse evaporative cooling system. *J. Arab Gulf Sci.* 21:71-8.
- Bailey B.J. 1981. The reduction of thermal radiation in glasshouses by thermal screens. *J. Agr. Eng. Res.* 26:215-24.
- Beyl C.A., Trigiano R.N. 2011. *Plant propagation concepts and laboratory exercises*, 2nd Ed. CRC Press, Boca Raton, FL, USA.
- Castellano S., Hemming S., Mohammadkhani G.R., Swinkels G.J.G., Mugnuzza G.S. 2010. Radiometric properties of agricultural permeable coverings. *J. Agric. Eng.* 41:1-12.
- Castellano S., Russo G., Mugnuzza G.S. 2006. The influence of construction parameters on radiometric performances of agricultural nets. *Acta Hort.* 718:283-90.
- Chen C., Shen T., Weng Y. 2011. Simple model to study the effect of temperature on the greenhouse with shading nets. *Afr. J. Biotechnol.* 10:5001-14.
- Cohen S., Fuchs M. 1999. Measuring and predicting radiometric properties of reflective shade nets and thermal screens. *J. Agr. Eng. Res.* 73:245-55.
- Cohen S., Möller M., Pirkner M., Tanny J. 2012. Measuring radiometric properties of screens used as crop covers. *International CIPA Conference 2012 on Plasticulture for a Green Planet 1015.*
- Cohen S., Möller M., Pirkner M., Tanny J. 2014. Measuring radiometric properties of screens used as crop covers. *Proc. Intl. CIPA Conference 2012 on Plasticulture for a Green Planet Acta Hort.* 1015:191-9.
- Gentle A.R., Dybdal, K.L., Smith, G.B. 2013. Polymeric mesh for durable infra-red transparent convection shields: applications in cool roofs and sky cooling. *Sol. Energy Mater. Sol. C.* 115:79-85.
- Gernot R. (Eds). 2008. *Primary processes of photosynthesis: principles and apparatus.* RSC Publishing, UK.
- Godbey L.C., Bond T.E., Zornig H.F. 1979. Transmission of solar and long-wavelength energy by materials used as covers for solar collectors and greenhouses. *Trans. ASAE.* 22:1137-44.
- Hemming S., Romero E.B., Mohammadkhani V., Breugel B.V. 2017. Energy saving screen materials: measurement method of radiation exchange, air permeability and humidity transport and a calculation method for energy saving. WUR, Netherlands.
- Kim Y.B., Lee S.Y., Jeong B.R. 2009. Analysis of the insulation effectiveness of the thermal insulator by the installation methods. *J. Bio-Env. Control.* 18:332-40.
- Kishore V.V.N. 2010. *Renewable energy engineering and technology: principles and practice*, Revised International Ed. TERI Press, New Delhi, India.
- Marshall R. 2016. *How to build your own greenhouse: designs and plans to meet your growing needs.* Storey Publishing, USA.
- Meijer J. 1980. Reduction of heat losses from greenhouses by means of internal blinds with low thermal emissivity. *J. Agric. Eng. Res.* 25:381-90.
- Na W.H., Lee J.W., Diop S., Lee H.W. 2013. Calculation of night sky temperature according to cloudiness in Daegu. *Curr. Res. Agric. Life Sci.* 31:40-6.
- Nijskens J., Deltour J., Coutisse S., Nisen A. 1985. Radiation transfer through covering materials, solar and thermal screens of greenhouses. *Agric. For. Meteorol.* 35:229-42.

- Nijskens J., Deltour J., Coutisse S., Nisen A. 1989. Radiometric and thermal properties of the new plastic films for greenhouse covering. *Acta Hort.* 245:71-7.
- Papadakis G., Briassoulis D., Mugnoz G.S., Vox G., Feuilloley P, Stoffers J.A. 2000. Review paper (se-structures and environment): radiometric and thermal properties of, and testing methods for, greenhouse covering materials. *J. Agr. Eng. Res.* 77:7-38.
- Ponce P., Molina A., Cepeda P., Lugo E., MacCleery B. 2014. *Greenhouse design and control.* CRC Press, London, UK.
- Rafiq A., Na W.H., Rasheed A., Kim H.T., Lee H.W. 2019. Determination of thermal radiation emissivity and absorptivity of thermal screens for greenhouse. *Prot. Hortic. Plant Factory* 28:311-21.
- Rafiq A., Na W.H., Rasheed A., Kim H.T., Lee H.W. 2020. Measurement of convective heat transfer coefficients of horizontal thermal screens under natural conditions. *Prot. Hortic. Plant Factory* 29:9-19.
- Rasheed A., Lee J.W., Lee H.W. 2018a. Evaluation of overall heat transfer coefficient of different greenhouse thermal screens using building energy simulation. *Prot. Hort. Plant Factory* 27:294-301.
- Rasheed A., Lee J.W., Lee H.W. 2018b. Development and optimization of a building energy simulation model to study the effect of greenhouse design parameters. *Energies.* 11:1-19.
- Rasheed A., Kwak C.S., Na W.H., Lee J.W., Kim H.T., Lee H.W. 2020. Development of a building energy simulation model for control of multi-span greenhouse microclimate. *Agronomy* 10:1236.
- Schettini E., Vox G., Lucia B.D. 2007. Effects of the radiometric properties of innovative biodegradable mulching materials on snapdragon cultivation. *Sci. Hortic.* 112:456-61.
- Sethi V.P., Sumathy K.C., Lee Pal D.S. 2013. Thermal modeling aspects of solar greenhouse microclimate control: a review on heating technologies. *Sol. Energy.* 96:56-82.
- Shukla A., Tiwari G.N., Sodha M.S. 2008. Experimental study of effect of an inner thermal curtain in evaporative cooling system of a cascade greenhouse. *Sol. Energy.* 82:61-72.
- Simpkins J.C., Mears D.R., Roberts W.J. 1976. Reducing heat losses in polyethylene covered greenhouses. *Trans. ASAE.* 19:714-9.
- Svensson L. 2014. Learn the basics of greenhouse climate control. Available from: <http://www.ludvigsvensson.com/climate-screens/tools/using-svensson-screens/climate-control-basics>
- Tanny J., Yisraeli Y., Cohen S., Schwartz A., Moreshet S., Grava A. 2006. Saving water by protecting banana plantation with shade nets: microclimatological and physiological effects. Final report of research project no. 304-0285-04.
- Willits D.H., Peet M.M. 2000. Intermittent application of water to an externally mounted, greenhouse shade cloth to modify cooling performance. *Trans. ASAE.* 43:1247-52.